Virus neutralization by germ-line vs. hypermutated antibodies

Ulrich Kalinke*, Annette Oxenius†, Constantino López-Macías‡, Rolf M. Zinkernagel, and Hans Hengartner

Institute of Experimental Immunology, 8091 Zurich, Switzerland

Contributed by Rolf M. Zinkernagel, June 19, 2000

Mice infected with vesicular stomatitis virus (VSV), a cytopathic virus closely related to rabies virus, mount a virus-neutralizing antibody response protecting against lethal disease. VSV-neutralizing monoclonal IgGs isolated from primary immune responses were devoid of somatic mutations, whereas most secondary and all hyperimmune response IgGs tested were hypermutated. A comparative analysis of recombinant single-chain antibody fragments (scFv-Cκ) revealed that even the germ-line precursor of one hypermutated antibody bound and neutralized VSV. Four somatic amino acid substitutions in V_H increased by 300-fold the binding strength of monovalent scFv-Cκ. The multivalent binding avidity of germ-line scFv-Cκ was increased by more than 10-fold compared with the monovalent binding strength. In contrast, hypermutated scFv-Cκ did not show such avidity effects. Thus the overall binding difference between the germ-line and the hypermutated VSV-neutralizing antibody was only 10- to 15-fold. This may explain why primary germ-line antibodies and secondary hypermutated antibodies directed against pathogens such as viruses and bacteria expressing repetitive antibody determinants show rather similar binding qualities, whereas monovalently binding hapten-specific antibodies can show ''affinity maturation'' effects of up to 1000-fold.

Neutralizing antibodies against many human pathogenic viruses such as polio virus, influenza virus, and rabies virus are generated early—i.e., within the first week after infection (1–7). Similarly, after infection of mice with vesicular stomatitis virus (VSV), a cytopathic unsegmented negative-strand RNA virus closely related to rabies virus (8), an early antibody response is observed, which can prevent dissemination of the virus to neuronal tissues and protects the host from a lethal progressive paralytic disease (9, 10). Within the first hours after VSV infection, when neutralizing antibodies are not yet induced, the interferon system critically contributes to the survival of mice (11, 12). As early as 2 days after infection, neutralizing antibodies are detectable in the serum (13). By 4 days after infection, hybridomas have been isolated that secrete VSV-neutralizing germ-line IgGs (14). All VSV-neutralizing antibodies analyzed were directed against one major antigenic site of the protein moiety of the viral glycoprotein (VSV-G) (14, 15).

The majority of primary response IgGs isolated 4 and 5 days after infection used V gene fragments of the heavy and the κ light chain (V_H and V_κ) belonging to the V_HQ52 and the V_κ19–28 gene families. These antibodies bound one defined subsite within the major antigenic site of VSV-G. In contrast, IgGs isolated from VSV-specific secondary and hyperimmune responses were predominantly V_H7183-positive and V_HJ558-positive (14). The comparison of VSV-specific monoclonal antibodies isolated from secondary and hyperimmune responses did not reveal evidence of further, drastic avidity increases or enhanced specific neutralizing capacities (16). The neutralizing capacity of primary-response IgGs isolated 4 and 5 days after immunization was reduced by 10- to 100-fold compared with secondary and hyperimmune response IgGs (14). Because no genealogically related germ-line and hypermutated antibodies were identified, it was unclear whether the increased neutralizing capacity of secondary and hyperimmune response IgGs was due to newly appearing antibody specificities binding to more efficiently neutralizing epitopes, or whether hypermutation had improved VSV-specific binding and neutralization of secondary and hyperimmune response IgGs.

To address this question, somatic variation of V_H7183-positive VSV-neutralizing monoclonal antibodies was analyzed. V_H sequence comparison of V_H7183/J_H2-positive antibodies revealed some amino acid substitutions, which were identical in different clones. The influence of these substitutions on VSV-specific binding and neutralization was studied in a comparative analysis of recombinant single-chain Fv-Cκ antibody fragments (scFv-Cκ) derived from one hypermutated antibody.

Materials and Methods

Mice and Viruses. Eight-week-old severe combined immunodeficient (SCID) BALB/c mice kept under specific pathogen-free conditions were obtained from Iffa Credo. VSV-IND (Mudd–Summers isolate) was originally obtained from D. Kolakofsky (University of Geneva, Switzerland) and was grown on BHK-21 cells (17).

Isolation and Sequencing of V_H and V_L Genes. The 7.8-kb *Eco*RI fragment encoding the functionally rearranged V_H of VI24 (pVH-VI24) was cloned from a λ-Zap library (Stratagene). V_Hs of other V_H7183/J_H2-positive hybridomas were isolated from cDNA by PCR, using the 5′ primer 1229 (5′-GAGTCTGGGGGAGGCTTAGT-3′) and the 3′ Cγ primer 1411 (5′-CCGATGGGGCTGTTGTTTTG-3′). V_L genes of VI26, VI30, VI22, and VI20 were amplified by using the 5′ V_κ21 primer 2225 (5′-TCCAGCTTCTTTGGCTGTGTCTCT-3′) and the 3′ C_κ primer 2236 (5′-ATGCTGTAGGTGCTGTCTTTGCTGT-3′). For V_L amplification of VI24, the 5′ V_κ8 primer 2224 (5′-GACATTGTGATGTCACAGTCTCCATCCTCCCTA-3′) and the 3′ C_κ primer 2335 (5′-TGTCGTTCATACTCGTCCTTGGTC-3′) were used. PCR products were gel purified and sequenced automatically (Applied Biosystems). The reliability of the reverse transcription–PCR approach was verified by identical V_H sequences obtained for VI24 by PCR cloning and genomic cloning.

Generation of scFv-Cκ Expression Constructs. V_H of VI24 was PCR amplified from pVH-VI24 by using the 5′ primer 1211

Abbreviations: VSV, vesicular stomatitis virus; VSV-G, VSV glycoprotein; scFv-Cκ, single-chain Fv-Cκ antibody fragments; SCID, severe combined immunodeficient; pfu, plaque-forming units; CDR, complementarity-determining region.

*To whom reprint requests should be sent at present address: EMBL Mouse Biology Program, Via E. Ramarini 32, 00016 Monterotondo Scalo (Roma), Italy. E-mail: kalinke@embl-monterotondo.it.

†Present address: Nuffield Department of Medicine, John Radcliffe Hospital, Oxford OX3 9DU, U.K.

‡Present address: Unidad de Investigación Médica en Immunoquímica, 1er piso Hospital de Especialidades, CMN s. XXI, IMSS, Av. Cuauhtémoc 330 col Doctores C.P. 06720, México D.F.

The publication costs of this article were defrayed in part by page charge payment. This article must therefore be hereby marked "*advertisement*" in accordance with 18 U.S.C. §1734 solely to indicate this fact.

(5′-TTTTGAGCTCACCATGGACTTCAGGCTCAATTTA-GTTTTCCTTGTCCT-3′) and the 3′ primer 3015 (5′-TAGGGAGGATGGAGACTGTGACATCACAATGT-CGTCGACTGAGGAGACTGTGAGAGTGGTGCC-3′). V_L was PCR amplified from cDNA, using the 5′ primer 2224 and the 3′ primer 2238 (5′-TTTTAAGCTTATACTTACGTTTTATT-TCCAGCTTGGTCCCCCCT-3). Using the flanking primers 1211 and 3015, we assembled the V_H and V_L PCR fragments and cloned them into pGEM-T (Promega). After sequence verification, the *Sst*I/*Hin*dIII fragment was ligated into a C_κ expression vector (18, 19). To construct a flexible linker between V_H and V_L, the primers 2119 (5′-TCGAAGGTGGAAGTGGAGGT-TCTGGTGGAAGTGGAGGTTCAGGTGGAG-3′) and 2120 (5′-TCGACTCCACCTGAACCTCCACTTCCACCAGA-ACCTCCACTTCCACCT-3′) (18) were annealed and ligated into the unique *Sal*I site between V_H and V_L (pscFv24-Cκ). Hypermutated V_H was reverted to germ-line by an oligonucleotide-directed mutagenesis approach. PCR fragments generated with the 5′ primer 1211 and a 3′ mutagenesis primer, consisting of the desired mutation flanked by 18 nucleotides at the 5′ and 3′ sides, and with the reverse complementary 5′ mutagenesis primer and the 3′ primer 1214 were PCR assembled and cloned into pGEM-T (Promega). After sequence verification the *Sst*I/*Sal*I fragment of pscFv24-Cκ was replaced by the mutagenized fragment. Complete germ-line sequence and the different intermediates were obtained by consecutive mutagenesis of V_H codons 31, 35, 58, and 99.

Expression of Recombinant scFv-Cκ Antibody Fragments. Stable transfectants were generated by protoplast fusion of J558L myeloma cells with *Escherichia coli* K803 transformed with various scFv-Cκ expression constructs. After subcloning, the transfectants were expanded in Iscove's modified Dulbecco's medium (10% FCS), and supernatant was collected. The scFv-Cκ concentration in the supernatant was determined by an ELISA, using affinity-purified scFv-Cκ protein as a standard. The concentration of purified scFv-Cκ was determined by A_{280} measurement and was verified by PAGE analysis. Proper splicing of recombinant scFv24-Cκ was validated by N-terminal protein sequencing, yielding the amino acid sequence DVQLV.

Quantification of VSV-Specific Binding of Recombinant scFv-Cκ Proteins. Supernatant of transfected hybridomas was serially 2-fold diluted and transferred to plates coated with purified VSV. After incubation for 1 h at room temperature, bound scFv-Cκ protein was detected by affinity-purified polyclonal horseradish peroxidase-labeled goat anti-mouse C_κ antibody (Southern Biotechnology Associates). To analyze binding avidity, supernatant containing scFv-Cκ protein was crosslinked by affinity-purified polyclonal horseradish peroxidase-labeled anti-mouse C_κ antibody (Southern Biotechnology Associates) for 30 min at room temperature before serial 2-fold dilution and transfer to VSV-coated plates.

VSV Neutralization Test. Samples were serially diluted by 2-fold and mixed with equal volumes of 50 plaque-forming units (pfu) of VSV. After incubation for 90 min at 37°C in an atmosphere containing 5% CO_2, 100 μl of the mixtures was transferred onto Vero cell monolayers in 96-well plates and incubated for 1 h at 37°C. The monolayers were overlaid with 100 μl of Dulbecco's modified Eagle's medium containing 1% methylcellulose. After incubation for 24 h at 37°C, the monolayer was stained with crystal violet. The dilution step reducing the number of plaques by 50% was taken as the titer (14).

Determination of *in Vivo* Protective Capacity of VSV-Neutralizing IgGs. SCID mice were i.p. injected with graded doses of purified monoclonal antibody in 1× PBS. After 5 h, when the antibody had disseminated in the diffusion volume of the mouse (about 3 ml), mice were infected i.v. with 10^8 pfu of VSV-IND. Four days later brains of surviving mice were assessed for the presence of virus. For this purpose brain tissue was homogenized in balanced salt solution, and serial 3-fold dilutions were plaqued on Vero cell monolayers in 96-well plates. Viral titers were calculated by multiplying counted plaques by the dilution factor. Mice without detectable virus in the brain ($<10^3$ pfu per brain) were scored as being protected (9).

Table 1. Neutralizing activity of V_H7183/J_H2-positive VSV-specific IgG monoclonal antibodies

Clone	Ig subclass	Neutralizing activity, titer·μg^{-1}·ml^{-1}*
Primary day 4		
41.6	IgG2a/κ	3
Secondary day 12		
VI26	IgG2a/κ	100
VI30	IgG2a/κ	100
VI22	IgG2a/κ	820
VI20	IgG3/κ	1,200
VI24	IgG2a/κ	800
Hyperimmune day 150		
VI53	IgG2a/κ	760
VI51	IgG3/κ	850
VI55	IgG2b/λ	330
VI52	IgG2a/κ	850
VI43	IgG2a/κ	680

*Neutralizing activity is expressed as the standardized neutralizing titer of monoclonal antibodies with a starting concentration of 1 μg/ml.

Results

V_H and V_L Sequence Comparison of VSV-Specific Monoclonal IgGs. To analyze somatic variation of IgGs representative for secondary and hyperimmune responses, the V_H and some V_L genes of 11 V_H7183/J_H2-positive VSV-neutralizing IgGs were isolated (Table 1). Sequence comparison revealed that all V_H7183/J_H2-positive IgGs used the same V_H61-1P germ-line gene fragment (20). Despite the use of the same V_H and J_H gene fragments, no common V_H-CDR3 motif was identified (Fig. 1*A*). The analyzed clones expressed various light chains consisting of three different J_κ segments and V_κ gene fragments belonging to four different V_κ gene families (Fig. 1*B*) (14). One clone (VI55) expressed a λ light chain (Table 1). The V_H sequence of the primary response clone 41.6 isolated 4 days after infection was devoid of somatic mutations (Fig. 1*A*). Similarly, the two sibling clones VI26 and VI30 isolated from a secondary response on day 12 after a booster infection on day 9 expressed germ-line sequences in both V_H and V_L (Fig. 1). The V_H and V_L regions of the secondary-response IgGs VI22 and VI20 were hypermutated, whereas only V_H but not V_L of VI24 showed somatic point mutations (Fig. 1). On average the analyzed secondary-response IgGs showed 1.6 somatic mutations per V_H region (range from 0 to 5). The V_H regions of all hyperimmune-response IgGs isolated on day 150 after repeated booster infections every 3 weeks were hypermutated and showed on average 8.8 somatic mutations (range from 3 to 18; Fig. 1*A*). Some of the somatic mutations encoded the same amino acid substitution at the same residue positions in different clones—i.e., mutations at codon 31 of V_H-CDR1 encoded a Ser^{31}-to-Asn substitution in the clones VI24, VI52, and VI43, and mutations at codon 55 in V_H-CDR2 encoded a Ser^{55}-to-Arg substitution in the clones VI22, VI53, VI51, VI55, and VI43 (Fig. 1*A*). It is interesting that the serine residues at positions 31 and 55 of the germ-line segment V_H61–1P are encoded by the putative mutational hotspot sequence AGC/T (25, 26).

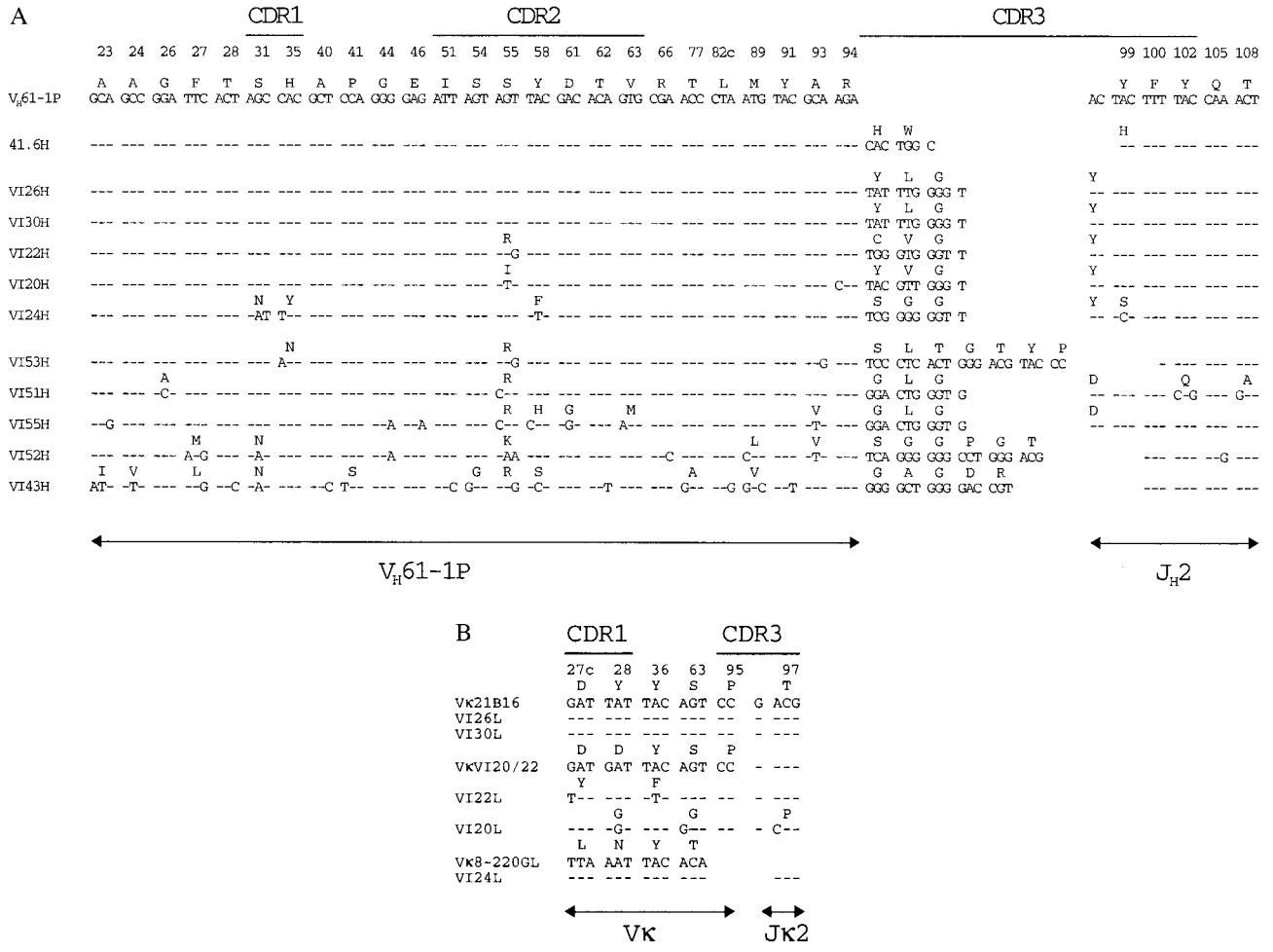

Fig. 1. Comparison of V_H and V_L sequences of V_H7183/J_H2-positive VSV-neutralizing antibodies. V_H and some V_L sequences of hybridomas are shown isolated from BALB/c mice 4 days after infection (41.6), isolated 12 days after primary infection and a booster infection on day 9 (VI26, VI30, VI22, VI20, and VI24), and isolated on day 150 after repeated booster infections every 3 weeks (VI53, VI51, VI55, VI52, and VI43). CDR, complementarity-determining region. (*A*) V_H sequences are aligned with germ-line sequences of the V_H61–1P gene (20) and the J_H2 segment (39). Only codons differing from the germ-line sequence are shown. V_H nucleotide sequence identity with reference sequences is indicated by - - -. Differences are marked by the respective nucleotide, and a change in the deduced amino acid is shown by the single-letter code. Codons are numbered according to ref. 22. (*B*) V_L sequences are aligned with the germ-line sequences of the $V_κ$21B16 gene (23), the $V_κ$8–220GL gene (24), and the $J_κ$2 segment (21). The $V_κ$ consensus sequence of VI20L and VI22L ($V_κ$VI20/22) is identical to an unrelated $V_κ$ sequence (accession no. AF045518) and presumably represents a previously undescribed germ-line gene of the $V_κ$21 family. The sequence data are available from the European Molecular Biology Laboratory nucleotide sequence database (accession nos. AJ400966–81).

VSV-Specific Binding of scFv-Cκ Antibody Fragments. To determine the influence of the V_H substitutions Ser^{31} to Asn and Ser^{55} to Arg on VSV-specific binding and neutralization, recombinant scFv24-Cκ were generated. The 38-kDa recombinant proteins consisted of the Fv portion of the mAb VI24 and the constant (C) domain of the κ light chain (Fig. 2 *A* and *C*). VI24 was chosen for this analysis because (*i*) VI24 expressed four somatic amino acid substitutions in V_H, one of which was the V_H Ser^{31}-to-Asn substitution; (*ii*) VI24 did not express the V_H Ser^{55}-to-Arg substitution, which allowed us to determine the influence of this substitution on the specificity of the VI24 germ-line precursor; and (*iii*) V_L of VI24 was devoid of somatic mutations, facilitating the mutational analysis. In parallel with scFv24-Cκ, related proteins were generated that expressed the complete germ-line sequence (M0), the V_H Ser^{31}-to-Asn substitution (M31), the V_H Ser^{55}-to-Arg substitution (M55), or both substitutions (M31.55) (Fig. 2*B*).

VSV-specific binding of the different scFv-Cκ antibody fragments was quantified in a standard solid-phase ELISA, using the cell culture supernatant of transfected myeloma cells. The germ-line scFv-Cκ M0 showed half-maximum binding at a concentration of approximately 3 μg/ml. Crosslinking by polyclonal anti-Cκ antibody improved binding of M0 by about 20-fold (Fig. 3*A*). Hypermutated scFv24-Cκ showed half-maximal VSV binding at a concentration of approximately 8 ng/ml, and crosslinking did not substantially improve the binding (Fig. 3*A*). Thus hypermutated scFv24-Cκ bound about 300-fold better than the putative germ-line precursor. However, crosslinked binding imitating binding of the complete antibody differed by only 10- to 15-fold.

The V_H Ser^{31}-to-Asn substitution in M31 reduced VSV-specific binding to an undetectable level. Crosslinked M31 showed a binding comparable to that of crosslinked M0 (Fig. 3*B*). The V_H Ser^{55}-to-Arg substitution in M55 not found in VI24 increased monovalent binding by about 10-fold compared with M0. Crosslinking improved the binding of M55 by 10-fold, resulting in an overall 3-fold reduced binding compared with hypermutated scFv24-Cκ (Fig. 3*C*). When both the Ser^{31}-to-Asn and the Ser^{55}-to-Arg substitutions were expressed, binding of M31.55 remained below that of M55; however, binding of crosslinked M31.55 was comparable to that of crosslinked M55 (Fig. 3*D*).

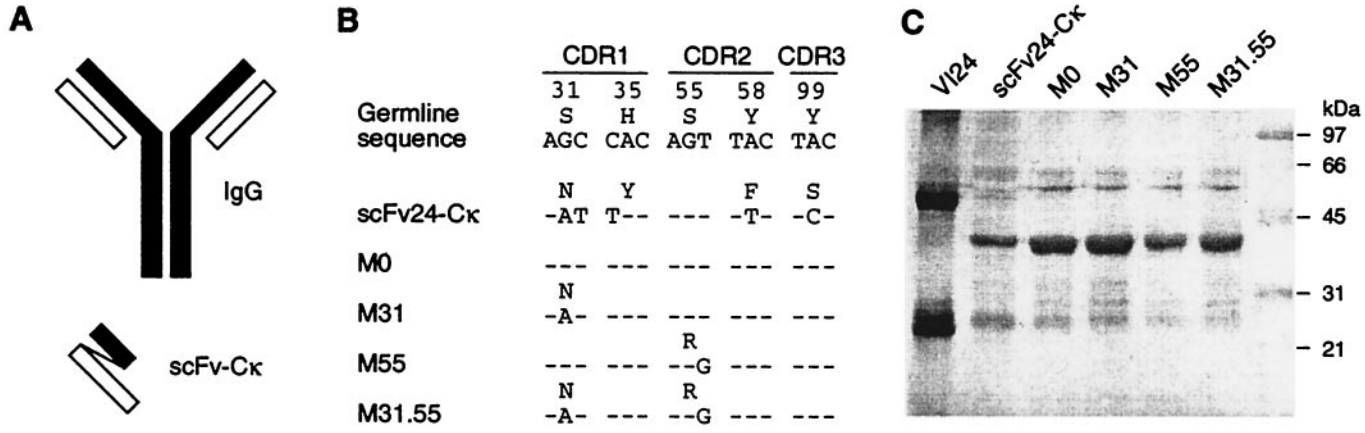

Fig. 2. Structural characteristics of the IgG VI24 and of recombinant scFv-Cκ. (*A*) Schematic diagram of a prototypical IgG (heavy chain, black; light chain, white) and of recombinant scFv-Cκ. In scFv-Cκ the carboxyl terminus of the V_H domain (black) is linked via the 18-aa linker [VE(GGS)$_4$GGVD] to the amino terminus of the κ light chain, consisting of the V_κ and the C_κ domains (white). (*B*) Sequence alignment of scFv24-Cκ derived from the parental antibody VI24 and of the scFv-Cκ derivatives M0, M31, M55, and M31.55. With the exception of the shown V_H codons 31, 35, 55, 58, and 99, sequences were identical (for notation and numbering see the legend of Fig. 1). The sequence data are available from the European Molecular Biology Laboratory nucleotide sequence database (accession nos. AJ400982–6). (*C*) SDS/PAGE analysis of purified VI24 and of purified scFv-Cκ proteins. Four micrograms of purified protein was separated by SDS/12% PAGE under reducing conditions and was visualized by silver staining (Bio-Rad). The IgG2a antibody VI24 gave rise to two bands, at 50 kDa for the heavy chain and at 25 kDa for the light chain. In contrast, the different scFv-Cκ proteins showed one major band at approximately 38 kDa, verifying the single-chain character of the proteins. In the last lane a prestained low-molecular-mass protein standard (Bio-Rad) was run.

VSV-Specific Neutralization by scFv-Cκ Antibody Fragments. To analyze whether the antibody VI24 gained the virus-neutralizing quality by "affinity maturation," various purified scFv-Cκ proteins and the parental antibody VI24, adjusted to a starting concentration of 50 μg/ml, were tested in a standard neutralization assay. Hypermutated scFv24-Cκ showed a neutralization titer of 5–6, which improved by 20-fold after crosslinking (Fig. 3*E*). Because crosslinking did not substantially increase binding, the enhanced neutralization of crosslinked scFv24-Cκ was probably due to the reduced viral cell adsorption, caused either by the induction of conformational changes in the viral envelope or simply by thickening of the protein layer covering the viral surface. Crosslinked scFv24-Cκ showed a 4-fold reduced neutralization compared with the parental antibody VI24, indicating that crosslinking by anti-C_κ antibody is a good approximation but not a complete imitation of steric conditions of bivalent IgG binding of VI24. Germ-line scFv-Cκ M0 showed a neutralizing titer of 3, whereas crosslinking improved neutralization by about 8-fold (Fig. 3*E*). Thus even the germ-line precursor of VI24 bound and neutralized VSV, and hypermutation improved neutralization of VI24 by about 15-fold. The neutralizing activity of monovalent M31 was below the detection level, which was in accordance with the absence of VSV-specific binding of monovalent M31 (Fig. 3*B*), whereas crosslinked M31 showed a neutralization that was 4-fold reduced compared with crosslinked M0. The V_H Ser^{55}-to-Arg substitution in M55 increased the neutralizing activity of crosslinked M55 by about 4-fold compared with crosslinked M0 (Fig. 3*E*). The neutralizing activity of M31.55 was comparable to that of M55 (Fig. 3*E*).

***In Vivo* Protective Capacity of Hypermutated vs. Germ-Line IgGs.** To test whether hypermutation played a role in reaching protective antibody serum levels, the *in vivo* protective capacity of hypermutated and germ-line IgGs was analyzed. Because of the short serum half-life, single-chain Fv antibody fragments were not suitable for *in vivo* analysis (11). Therefore SCID mice were reconstituted with graded doses of purified monoclonal IgGs, and 5 h later mice were infected i.v. with 10^8 pfu of VSV-IND. After 4 days, brains of surviving mice were assessed for the presence of virus. Surviving SCID mice lacking detectable virus titers in the brain were scored as being protected.

As shown earlier, hypermutated VSV-neutralizing antibodies isolated from secondary and hyperimmune responses protected 50% of the SCID mice at concentrations between 5 and 10 μg per mouse (Fig. 4, closed symbols; see also ref. 9). Similarly, the germ-line antibody VI26 isolated from a secondary response protected 50% of the SCID mice at a concentration of approximately 10 μg per mouse (Fig. 4*B*, open squares). Germ-line antibodies isolated from early primary responses protected SCID mice at concentrations ranging from 20 μg per mouse (antibody 51.3, Fig. 4*B*, open triangles) to >100 μg per mouse (antibody 41.11, Fig. 4*A*, open squares). Similar conditions were found for V_HQ52/Vκ19-28-positive and V_H7183/J_H2-positive VSV-neutralizing IgGs (Fig. 4).

Discussion

This study evaluated the influence of single and combined somatic amino acid substitutions in V_H of one hypermutated VSV-neutralizing antibody on VSV-specific binding and neutralization. Primary-response VSV-neutralizing IgGs were devoid of somatic mutations, whereas most secondary and all hyperimmune-response IgGs tested showed somatic mutations (on average 1.6 and 8.8 mutations per V_H region, respectively). The analysis of V_H7183/J_H2-positive IgGs representative for secondary and hyperimmune responses against VSV indicated that all neutralizing IgGs tested used one particular V_H germline gene fragment (V_H61–1P). Because of the particle nature of VSV (diameter of 65 nm and length of 180 nm) and the repetitiveness of the glycoprotein on the viral surface (1,200 VSV-G per virion) (8), on and off rates of VSV-specific antibody binding could not be determined directly by in-solution equilibrium methods. To determine the influence of two commonly found amino acid substitutions in V_H on virus-specific binding in a solid-phase ELISA, recombinant antibody fragments displaying one antigen-specific site per molecule were generated (scFv-Cκ). Crosslinking of scFv-Cκ by anti-C_κ antibody before analysis in a solid-phase ELISA allowed quantification of avidity effects by multivalent binding.

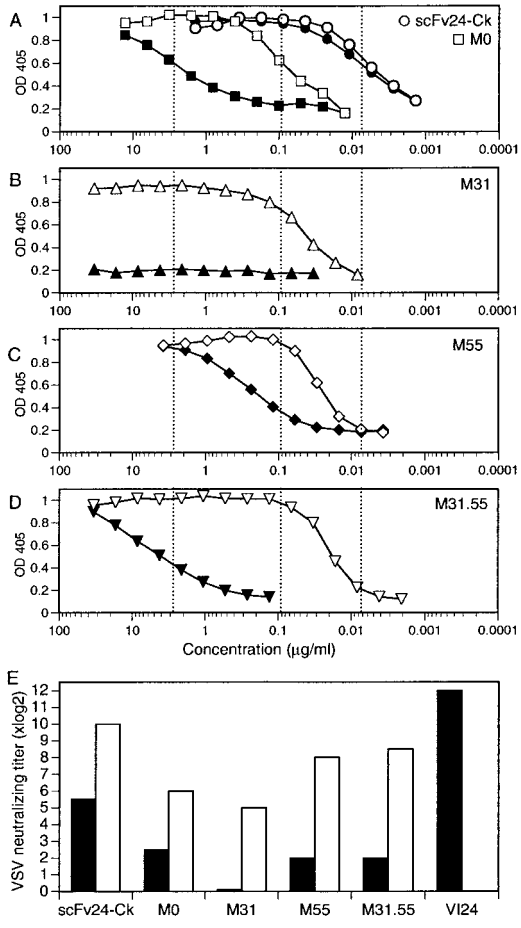

Fig. 3. VSV-specific binding and neutralization of scFv-Cκ antibody fragments. Supernatant containing scFv-Cκ protein was serially 2-fold diluted and transferred to VSV-coated plates. Bound scFv-Cκ was detected by horseradish peroxidase-labeled anti-C_κ antibody (closed symbols). To determine avidity effects, supernatant containing scFv-Cκ was crosslinked by horseradish peroxidase-labeled anti-C_κ antibody before serial 2-fold dilution and then applied to VSV-coated plates (open symbols). (*A*) VSV-specific binding of hypermutated scFv24-Cκ (circles) and of germ-line scFv-Cκ M0 (squares). (*A–D*) Half-maximal binding of scFv24-Cκ and M0 is indicated by dotted lines. (*B*) The V_H Ser^{31}-to-Asn substitution did not improve scFv-Cκ binding. (*C*) Despite the fact that the V_H Ser^{55}-to-Arg substitution was not expressed by the parental antibody VI24, it improved the binding of M55. (*D*) Coexpression of the V_H Ser^{31}-to-Asn and the V_H Ser^{55}-to-Arg substitutions improved binding of M31.55. (*E*) VSV-IND neutralization by various scFv-Cκ antibody fragments was tested with untreated reagents (black bars) and after crosslinking (open bars). For crosslinking, 2.5 μg of purified scFv-Cκ protein was incubated with 1.25 μg of anti-C_κ antibody in a total volume of 100 μl for 30 min at room temperature. The crosslinked and untreated scFv-Cκ protein and the purified antibody VI24 were serially 2-fold diluted and analyzed in a standard neutralization assay. The protein dilution reducing the number of plaques by 50% is indicated as the titer.

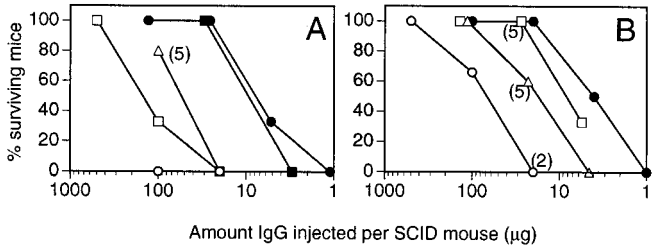

Fig. 4. Protective capacity of hypermutated and germ-line IgGs in mice. SCID mice were reconstituted with graded doses of monoclonal antibodies of the IgG2a subclass, which were either devoid of somatic mutations (open symbols) or hypermutated (filled symbols). Five hours later mice were i.v. challenged with 10^8 pfu of VSV-IND. After 4 days the brains of surviving mice were assessed for the presence of virus. Mice without detectable virus were scored as being protected. Groups of three mice were tested; deviating numbers of tested animals are given in parentheses. (*A*) Analysis of IgGs using V gene fragments belonging to the V_HQ52 and the V_κ19–28 families. The germ-line antibodies 41.11 (□), 41.2 (△), and 41.9 (○) were isolated from primary responses 4 days after infection. The hypermutated antibodies VI10 (■) and VI49 (●) were isolated, respectively, from a secondary response 12 days after infection and from a hyperimmune response 150 days after infection. (*B*) Analysis of IgGs using the V_H61–1P germ-line gene fragment belonging to the V_H7183 family and the J_H2 segment. The germ-line antibodies 41.6 (□) and 51.3 (△) were isolated from primary responses 4 and 5 days after infection, respectively. The germ-line antibody VI26 (□) was isolated from a secondary response 12 days after infection. The hypermutated antibody VI43 (●) was isolated from a hyperimmune response 150 days after infection.

VSV-specific binding of the hypermutated scFv24-Cκ was improved by 300-fold compared with the germ-line precursor M0. Crosslinking improved binding of the germ-line precursor M0 by about 20-fold but did not substantially change binding of hypermutated scFv24-Cκ. Thus, avidity effects enhancing only the binding of the VI24 germ-line precursor led to an overall 10- to 15-fold improved binding of the hypermutated antibody VI24.

The Ser^{55}-to-Arg substitution, not found in the parental antibody VI24 but expressed by 50% of the analyzed secondary and hyperimmune IgGs, was achieved by either an A-to-C transition at the first base (clones VI51 and VI55) or a T-to-G transition at the third base (clones VI22, VI53, and VI43). These mutations differed from intrinsic hypermutation patterns (25) and therefore might have been antigen driven. Indeed, the Ser^{55}-to-Arg substitution improved binding and neutralization of the VI24 germ-line precursor antibody by 10- to 15-fold, indicating an independent second way of improving the VI24 germ-line precursor. Similar to the V_H-Trp^{33}-to-Leu substitution in V186.2V_H/Vλ1-positive 4-hydroxy-3-nitrophenylacetyl (NP)-specific antibodies (27), the Ser^{55}-to-Arg substitution presumably is indicative of "affinity maturation" of V_H7183/J_H2-positive VSV-specific antibodies.

The G-to-A transition at the second base of the V_H codon 31 of VI24, VI52, and VI43 encoding the Ser^{31}-to-Asn substitution was introduced at a mutational hot spot sequence and resembled a pattern found at codon 31 of the V_κOX1 transgenic light chain, which was caused by the preferred intrinsic specificity of the hypermutation mechanism (25). This suggested that the V_H Ser^{31}-to-Asn mutation in VI24 might not have been selected on the basis of improved VSV binding. Indeed, expression of the Ser^{31}-to-Asn substitution reduced monovalent binding below the detection level, whereas multivalent binding remained unaltered. The more peripheral localization of V_H Asn^{31} might have caused a paratope twist during monovalent binding, whereas during multivalent binding the paratope was forced into a better fitting position, thus allowing binding.

A computer model of the solvent-accessible surface of the Fv domain of VI24 showed a combining site forming a shallow groove along the V_H–V_L interface (data not shown). The central area of the groove was located between V_H-CDR2 and V_L-CDR1. The relatively short lengths of V_H-CDR3 and V_L-CDR3 caused V_H-CDR1 and -2 and V_L-CDR1 to "stick out," whereas V_L-CDR2 seemed to be too remote to be a significant part of the binding site. The V_H Asn^{31}, Ser^{55}, and Phe^{58} residues were solvent exposed and probably were part of the anticipated binding domain, whereas V_H Tyr^{35} was only partially accessible. The V_H Ser^{99} residue was buried and packed against the base of V_L-CDR1 and -CDR2. V_H Ser^{99} presumably is not part of the binding domain and probably has an indirect role in inducing or stabilizing the V_H-CDR3 conformation.

The antigen-combining site of protein-specific antibodies usually comprises a surface of about 700 $Å^2$ (28). Affinity maturation of protein-specific antibodies typically results in a 10-fold (29) and, in a few cases, in about a 100-fold improved binding strength (30). In contrast, the antibody surface involved in hapten-specific binding usually is considerably smaller (approximately 25%). Therefore hapten-specific antibodies may accumulate replacement mutations in the V region, including parallel ones, which do not contribute to binding and thus do not affect the binding strength (27, 28). A 10-fold affinity increase after one amino acid substitution was observed for a phenyloxazolone-specific antibody (31), whereas three amino acid substitutions in V_H of a *p*-azophenylarsonate-specific antibody increased the affinity 200-fold (32). We found a 300-fold-improved binding strength of the hypermutated Fv domain of an antibody binding the protein moiety of VSV-G and an overall improvement of the complete antibody by 10- to 15-fold. It is interesting that even the VI24 germ-line precursor antibody neutralized VSV, as did all other primary-response germ-line antibodies analyzed (14). This observation raised the question of whether germ-line antibodies were effective in protection against a lethal VSV infection and what role affinity maturation may have in controlling cytopathic viral infections.

Protection experiments indicated that three hypermutated antibodies tested protected at concentrations of about 2.5 μg/ml, which was in accordance with previous results (9) and similar to prophylactic antibody doses against rabies virus and mouse influenza virus infection (3 μg/ml and 1–20 μg/ml, respectively; refs. 33 and 34). Four of the analyzed primary-response VSV-neutralizing germ-line antibodies protected at concentrations of 15 μg/ml, and one (51.3) protected at a concentration of about 4 μg/ml. Thus five of six primary-response antibodies tested in this study protected from a lethal VSV infection at about a 10-fold higher concentration than secondary- and hyperimmune-response antibodies. Because in the acute phase of the Ig response up to 10% of the total Ig theoretically can be antigen-specific (35), critical serum levels sufficient for protection can be reached by germ-line antibodies at early times after infection. For later times, when lower percentages of serum Ig are antigen-specific, it can be advantageous that the protective capacity of antibodies is increased.

Since this study focused on the analysis of one particular antibody isolated form one specific mouse strain (BALB/c), further experiments are required to draw general conclusions. However, our data are compatible with previous results (14), including the observation of natural VSV-neutralizing antibodies in the serum of uninfected mice (36, 37), suggesting the following scenario taking place after VSV infection *in vivo*: Free virus particles bind and crosslink B cell receptors of naive red pulp B cells, leading to secretion of mostly $V_HQ52/V_\kappa19–28$-positive VSV-neutralizing germ-line antibodies. The stimulation of primarily one B cell subpopulation correlates with the skewed expression of V_HQ52 in the naive B cell repertoire (14) and might be driven by VSV-G subepitopes expressed on the surface of free virus particles particularly accessible for $V_HQ52/V_\kappa19–28$-positive antibodies. Later and after repeated immunizations, VSV-specific B cells expressing antibodies composed of various V_H elements belonging to different gene families, including the V_H7183 and V_HJ558 gene families, are predominantly found in germinal centers. B cell receptors of germinal center B cells are hypermutated and selected for retained or improved VSV-specific binding by VSV-G presented on follicular dendritic cells (38). Because on the surface of free virus particles VSV-G is expressed in a highly organized form, whereas on follicular dendritic cells VSV-G is presented in a less ordered form (38), it is likely that hypermutated B cell receptors with improved monovalent binding properties are selected in the germinal centers. A mechanism replacing early neutralizing antibodies with new types of hypermutated antibodies with only marginally improved binding qualities could be that V_H7183-positive and V_HJ558-positive precursors sustained extensive hypermutation better than V_HQ52-positive precursors without losing VSV specificity.

We thank Therese Uhr for expert technical assistance; Dieter Zimmermann for providing the sequencing service; Ariel van der Bent and Annemarie Honegger for computer modeling of the VI24 Fv domain; Peter Hunziker for the amino-terminal sequencing of the scFv24-Cκ protein; and Alain Lamarre, Martin F. Bachmann, and Andrew McPherson for critical reading of the manuscript. This work was supported by grants from the Swiss National Foundation, the Canton of Zurich, and the Deutsche Forschungsgemeinschaft (KA 990/1-1).

1. Dietzschold, B., Rupprecht, C. E., Fu, Z. F. & Koprowski, H. (1996) in *Virology*, eds. Fields, B. N., Knipe, D. M. & Howley, P. M. (Lippincott-Raven, Philadelphia), Vol. 1, pp. 1137–1159.
2. Klenk, H. D. & Rott, R. (1988) *Adv. Virus Res.* **34,** 247–281.
3. Ogra, P. L., Fishaut, M. & Gallagher, M. R. (1980) *Rev. Infect. Dis.* **2,** 352–369.
4. Sabin, A. B. (1981) *Rev. Infect. Dis.* **3,** 543–564.
5. Ueki, Y., Goldfarb, I. S., Harindranath, N., Gore, M., Koprowski, H., Notkins, A. L. & Casali, P. (1990) *J. Exp. Med.* **171,** 19–34.
6. Webster, R. G. & Rott, R. (1987) *Cell* **50,** 665–666.
7. Zinkernagel, R. M. (1996) *Science* **271,** 173–178.
8. Wagner, R. R. (1987) *The Rhabdoviruses* (Plenum, New York).
9. Bachmann, M. F., Kalinke, U., Althage, A., Freer, G., Burkhart, C., Roost, H., Aguet, M., Hengartner, H. & Zinkernagel, R. M. (1997) *Science* **276,** 2024–2027.
10. Lefrancois, L. (1984) *J. Virol.* **51,** 208–214.
11. Kalinke, U., Krebber, A., Krebber, C., Bucher, E., Pluckthun, A., Zinkernagel, R. M. & Hengartner, H. (1996) *Eur. J. Immunol.* **26,** 2801–2806.
12. Steinhoff, U., Muller, U., Schertler, A., Hengartner, H., Aguet, M. & Zinkernagel, R. M. (1995) *J. Virol.* **69,** 2153–2158.
13. Bachmann, M. F., Kundig, T. M., Kalberer, C. P., Hengartner, H. & Zinkernagel, R. M. (1994) *J. Immunol.* **152,** 4235–4241.
14. Kalinke, U., Bucher, E. M., Ernst, B., Oxenius, A., Roost, H. P., Geley, S., Kofler, R., Zinkernagel, R. M. & Hengartner, H. (1996) *Immunity* **5,** 639–652.
15. Roost, H. P., Haag, A., Burkhart, C., Zinkernagel, R. M. & Hengartner, H. (1996) *J. Immunol. Methods* **189,** 233–242.
16. Roost, H. P., Bachmann, M. F., Haag, A., Kalinke, U., Pliska, V., Hengartner, H. & Zinkernagel, R. M. (1995) *Proc. Natl. Acad. Sci. USA* **92,** 1257–1261.
17. McCaren, L. C., Holland, J. J. & Syverton, J. T. (1959) *J. Exp. Med.* **109,** 475–485.
18. Traunecker, A., Lanzavecchia, A. & Karjalainen, K. (1991) *EMBO J.* **10,** 3655–3659.
19. Traunecker, A., Oliveri, F. & Karjalainen, K. (1991) *Trends Biotechnol.* **9,** 109–113.
20. Chukwuocha, R. U., Hartman, A. B. & Feeney, A. J. (1994) *Immunogenetics* **40,** 76–78.
21. Sakano, H., Huppi, K., Heinrich, G. & Tonegawa, S. (1979) *Nature (London)* **280,** 288–294.
22. Kabat, E., Wu, T. T., Perry, H. M., Gottesman, K. S. & Foeller, C. (1991) *Sequences of Proteins of Immunological Interest.* (U.S. Department of Health and Human Services, Bethesda, MD), 5th Ed.
23. Heinrich, G., Traunecker, A. & Tonegawa, S. (1984) *J. Exp. Med.* **159,** 417–435.
24. Clarke, S. & McCray, S. (1991) *J. Immunol.* **146,** 343–349.
25. Betz, A. G., Rada, C., Pannell, R., Milstein, C. & Neuberger, M. S. (1993) *Proc. Natl. Acad. Sci. USA* **90,** 2385–2388.
26. Rogozin, I. B. & Kolchanov, N. A. (1992) *Biochim. Biophys. Acta* **1171,** 11–18.
27. Allen, D., Simon, T., Sablitzky, F., Rajewsky, K. & Cumano, A. (1988) *EMBO J.* **7,** 1995–2001.
28. Davies, D. R., Padlan, E. A. & Sheriff, S. (1990) *Annu. Rev. Biochem.* **59,** 439–473.
29. Roberts, S., Cheetham, J. C. & Rees, A. R. (1987) *Nature (London)* **328,** 731–734.
30. Clarke, S., Rickert, R., Wloch, M. K., Staudt, L., Gerhard, W. & Weigert, M. (1990) *J. Immunol.* **145,** 2286–2296.
31. Berek, C. & Milstein, C. (1987) *Immunol. Rev.* **96,** 23–41.
32. Sharon, J. (1990) *Proc. Natl. Acad. Sci. USA* **87,** 4814–4817.
33. Dietzschold, B., Gore, M., Marchadier, D., Niu, H. S., Bunschoten, H. M., Otvos, L., Jr., Wunner, W. H., Ertl, H. C., Osterhaus, A. D. & Koprowski, H. (1990) *J. Virol.* **64,** 3804–3809.
34. Mozdzanowska, K., Furchner, M., Washko, G., Mozdzanowski, J. & Gerhard, W. (1997) *J. Virol.* **71,** 4347–4355.
35. Funk, G. A., Barbour, A. D., Hengartner, H. & Kalinke, U. (1998) *J. Theor. Biol.* **195,** 41–52.
36. Gobet, R., Cerny, A., Ruedi, E., Hengartner, H. & Zinkernagel, R. M. (1988) *Exp. Cell. Biol.* **56,** 175–180.
37. Ochsenbein, A. F., Fehr, T., Lutz, C., Suter, M., Brombacher, F., Hengartner, H. & Zinkernagel, R. M. (1999) *Science* **286,** 2156–2159.
38. Bachmann, M. F. (1998) *Immunol. Res.* **17,** 329–344.
39. Sakano, H., Maki, R., Kurosawa, Y., Roeder, W. & Tonegawa, S. (1980) *Nature (London)* **286,** 676–683.